THE CALCULATION OF THE FREE FIELD RESPONSE OF A CANYON

Boyan ZHANG*

In this paper, the analysis procedures of determining the free field response of a canyon are described, and the basic equation of motion of a canyon free field response is established, in which the coupling method of finite element and infinite element is adopted. The infinite element aspects are presented in detail, including the element classification, the convergence of the stiffness matrices, the numerical integration scheme. A test example is given to demonstrate the accuracy of the method, and an engineering application of the use of the elements for solving free field seismic motions at arch dam canyon is given.

Key Words : *infinite elements, numerical integration, free-field seismic motion*

1. INTRODUCTION

The earthquake input mechanism is an important topic in the dynamic analysis of large arch dams, where the key point is to determine the canyon free field seismic motion. But, spatial variations in earthquake motion around the canyon have rarely been considered in practice. At present, the standard earthquake input mechanism[1] is still used in engineering, in which a free field earthquake accelerogram recorded at ground surface is applied identically to the deformable dam foundation interface. It will result in the same motion acts at all points along the interface, and the deformable foundation is assumed to be massless to avoid both the artificial amplification of earthquake waves inputted to the dam structure and the pseudo foundation vibration modes which may dominate the dynamic response of the dam. In fact, the massless dam foundation is not substantial and the earthquake motion along the canyon at the dam site should not be uniform. A small amount of earthquake records measured on the canyon both banks indicate that earthquake motions around the canyon habe considerable spatial variations. And yet, for an arch dam, a slight change of the distance between its abutments has a great influence on its stress distribution. Therefore the free field response of a cayon must be investigated.

The calculation of the canyon free field seismic motion has been receiving attention in recent years. Analysis solutions to the semi-circular and semi-elliptical canyons in a homogeneous half space for the out-of-plane motion (*SH* waves)

have been given[2,3]. For more general cases, various numerical techniques have been developed, including the finite element method[4], generalized inverse method[5], wave function expansion method[6], boundary element method[7,8]. And the key problem of determining canyon free field motion is the numerical simulation of the unbounded domain. Conceptually, infinite element method seems to be simple and easy for solutions of infinite continuum problems.

The conception of the infinite elements is first suggested by Bettess and Zienkiewicz[9,10]. The method has now been applied successfully to a wide range of fields. For example, in the study of fluid-structure interaction[10] and underground excavation[11] problems, as well as in the analysis of strip foundation wave problems[12] and effects of canyon topography and geological conditions on strong ground motion[13]. But the numerical integration method is not perfect in Ref 12) and Ref 13), and the application of this method in practical dam engineering is seldom seen. This paper will give an improving result on the numerical integration scheme, and a modified coupling model of finite and infinite elements is used to determine the free field response of a canyon. In order to reduce computational cost, it is assumed that the canyon has a uniform cross-section to infinity and that the incident waves propagate normal to the axis of the canyon, so the two-dimensional models for the out-of-plane response to *SH* waves and the in-plane response to *P* and *SV* waves can be adopted to replace the three dimensional prototype valley. Besides, assuming the canyon foundation is subjected to a harmonic load and the medium possesses a linear property. Hence, the law of superposition is valid, and the analysis is performed

* M. Eng. Engineer, Dept. of Earthquake Engineering, Institute of Water Conservancy and Hydroelectric Power Research, P.O. Box 366, Beijing P.R. China
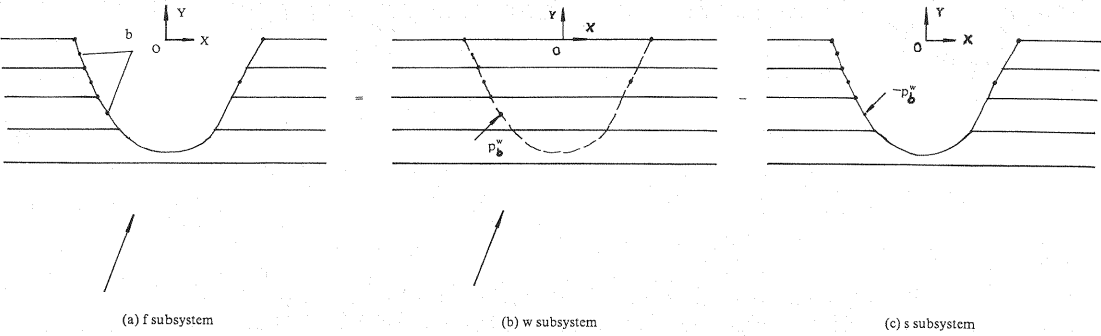
| (a) f subsystem | (b) w subsystem | (c) s subsystem |

Fig.1 The calculation model of the free field response of a canyon

in frequency domain, the *FFT* technique is also used in the calculation for the transient motion.

2. ANALYSIS PROCEDURES AND FORMULATIONS

Determining the free field response of a canyon can be illustrated in **Fig.1**, in which the signs *f*, *w* and *s* are adopted to distinguish the different subsystems. Because it is assumed that the medium has a linear property, the law of superposition is available and so the equation of motion for the nodes on canyon boundary is formulated as

$$\{u_b^f\} = \{u_b^w\} - \{u_b^s\} \quad \cdots\cdots\cdots\cdots\cdots\cdots (1)$$

where the subscript *b* represents the nodes on both the canyon boundaries for *f* and *s* subsystems and the fictitious canyon boundary for *w* subsystem (without canyon), so the analysis procedures can be divided into three parts as follows : First, the displacement amplitude vector $\{u_b^w\}$ for *w* subsystem is computed, and the node force vector $\{p_b^w\}$ is also formed. Second, the motion for *s* subsystem subjected to node load vector $-\{p_b^w\}$ is determined by the coupling model of finite element and infinite element that will simulate the effect of the unbounded soil region. Finally, the canyon free field motions under the earthquake excitation are obtained by the superposition as shown in Eq. (1).

（1） **the response of *w* subsystem**

The types of seismic waves considered are vertically propagating *P* and *S* waves in a layered half space. The displacement amplitude vector $\{u_b^w\}$ and the amplitude vector of the fictitious canyon boundary traction $\{t\}$ are computed by the method presented in Ref 19). for both vertically propagating *P* and *S* waves. The known three components of recorded accelerogram obtained at a horizontally layered half space can be separately calculated as three one-dimentional problems, in which the following one-dimensional wave motion equation with corresponding boundary conditions applies to every layer soil.

$$\rho \frac{\partial^2 u}{\partial t^2} = \mu \frac{\partial^2 u}{\partial y^2} + \eta_v \frac{\partial^3 u}{\partial y^2 \partial t} \cdots\cdots\cdots\cdots\cdots (2)$$

where ρ, η_v are mass density and viscous damping factor respectively, for horizontal component and vertical component, μ represents shear modulus and Young's modulus respectively.

Let $u(y, t) = U(y) e^{i\omega t}$, then Eq.(2) becomes an ordinary differential equation, solving the ordinary differential equation yields $\{u_b^w\}$ and $\{t\}$. The node load vector $\{p_b^w\}$ is formulated as :

$$\{p_b^w\} = \int_\Gamma [\bar{N}]^T \{t\} ds \cdots\cdots\cdots\cdots\cdots (3)$$

in which Γ represents the fictitious canyon boundary, $[\bar{N}]$ is the shape function matrix of the finite elements.

（2） **the response of *S* subsystem**

S subsystem is subjected to the node load vector $-\{p_b^w\}$ as shown in **Fig.1**(c), in which the near field is meshed by the standard finite elements and the far field is discretized by the infinite elements, so the subsystem's motion equation is :

$$\begin{bmatrix} S_{bb} & S_{br} \\ S_{rb} & S_{rr} \end{bmatrix} \begin{bmatrix} u_b^s \\ u_r^s \end{bmatrix} = - \begin{bmatrix} p_b^w \\ 0 \end{bmatrix} \cdots\cdots\cdots\cdots (4)$$

where $\{u_b^s\}$ and $\{u_r^s\}$ represnt the displacement amplitude vectors related to the canyon boundary nodes and remaining ones respectively. By using the condensation technique, Eq.(4) can be rewritten as :

$$[S_{bb}^s] \{u_b^s\} = - \{p_b^w\} \cdots\cdots\cdots\cdots\cdots (5)$$

in which

$$[S_{bb}^s] = [S_{bb}] - [S_{br}] [S_{rr}]^{-1} [S_{rb}] \cdots\cdots\cdots (6)$$

in Eq.(4) the dynamic-stiffness matrices $[S]$ are assembled from finite element and infinite element submatrices that have the expression as Eq.(7).

$$[S] = [K] (1 + i\eta_d) - \omega^2 [M] \cdots\cdots\cdots\cdots (7)$$

in which η_d is the hysteretic damping coefficient of the medium, ω is the exciting frequency, $[K]$, $[M]$ represent the static-stiffness and mass matrix respectively. Because the finite element is well
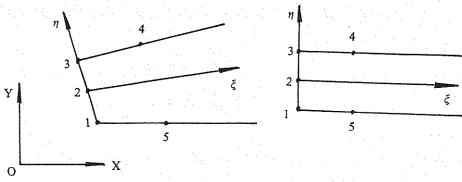
Fig.2 The 2-D dynamic infinite element

known[15], only the necessary statements about the infinite elements are given here.

(3) the canyon free field seismic motion

From Eqs.(1), (3) and (5), the basic equation of a canyon free field motion can be obtained :

$$\{u_b^f\} = \{u_b^w\} + [S_{bb}^s]^{-1}\{p_b^w\} \quad\cdots\cdots\cdots\cdots\cdots (8)$$

3. INFINITE ELEMENTS

(1) convergence

Infinite elements are the radiate narrow bands that extend to infinite, which are sketched in **Fig.2**. Their shape functions have many possible choices for different problems. In this paper, we adopt the mapping and shape functions which are employed in Ref.12) and Ref.13).

Mapping functions for coordinate transform :

$$
\left.
\begin{aligned}
&M_1 = \frac{1}{2}(1-\zeta)(1-\eta), \quad M_2 = 0 \\
&M_3 = \frac{1}{2}(1+\eta)(1-\zeta), \quad M_4 = \frac{1}{2}(1+\eta)\zeta \\
&M_5 = \frac{1}{2}(1-\eta)\zeta
\end{aligned}
\right\}
$$
$$\cdots\cdots\cdots\cdots\cdots\cdots\cdots\cdots\cdots (9)$$

Shape functions for displacement transform :

$$
\left.
\begin{aligned}
&N_1 = \frac{1}{2}P(\zeta)\eta(\eta-1) \\
&N_2 = P(\zeta)(1-\eta)(1+\eta) \\
&N_3 = \frac{1}{2}P(\zeta)\eta(\eta+1)
\end{aligned}
\right\}
\cdots\cdots\cdots\cdots (10)
$$

where $P(\zeta)$ is called the propagation function

$$P(\zeta) = \exp[-(\alpha+i\beta)\zeta] \quad\cdots\cdots\cdots\cdots (11)$$

where α is an amplitude decay facter due to wave dispersion, $\beta = \omega/c$ is the wave number describing the phase delay due to wave propagation. The infinite elements defined here have the following characteristic[12] : (1) the displacement compatibility on the interface between finite and infinite elements ; (2) the displacement continuity along the common boundary of neighbouring infinite elements. Hence, they can be used to simulate a stratified canyon foundation.

Infinite element's stiffness matrix can be written as

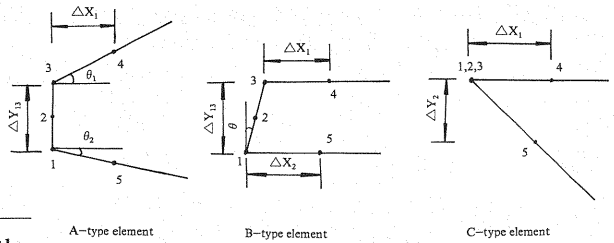$$[K]_{ij} = \int_0^\infty \int_{-1}^1 [B]_i^T[D][B]_j \det[J] d\eta d\zeta$$

Fig.3 The classification of infinite elements

$$= \int_0^\infty \int_{-1}^1 [K_{ij}] \frac{P^2(\zeta)}{\det[J]} d\eta d\zeta \cdots\cdots\cdots (12)$$

in which $[B]_i$ and $[B]_j$ are the strain sub-matrices, $[D]$ is an elasticity matrix containing the appropriate material properties, $\det[J]$ is the Jacobian determinant. All the elements of $[K_{ij}]$ are polynomial functions relating to ζ and η. The convergence of the stiffness matrices depends on the forms of the integrands which are decided by the shapes of the infinite elements, and therefore the elements are divided into three classifications as shown in **Fig.3**.

For A-type infinite elements, $\det[J]$ is

$$\det[J]_A = \frac{1}{2}\Delta X_1 \Delta Y_{13}(1+m\zeta) \cdots\cdots\cdots\cdots (13)$$

$$m = \frac{1}{\Delta Y_{13}}\Delta X_1(tg\theta_1 + tg\theta_2) \cdots\cdots\cdots\cdots\cdots (14)$$

For B and C-type element, we acquire $\det[J]_B$ and $\det[J]_C$ respectively

$$\det[J]_B = \frac{1}{4}\Delta Y_{13}[(\Delta X_1 + \Delta X_2)$$
$$+\eta(\Delta X_1 - \Delta X_2)] \cdots\cdots\cdots\cdots (15)$$

$$\det[J]_C = \frac{1}{2}\Delta X_1 \Delta Y_2 \zeta \cdots\cdots\cdots\cdots\cdots\cdots (16)$$

According to the above-mentioned analysis, the calculation of infinite element stiffness matrices involves the integration in η and ζ directions. For A, B, C-type elements, the integration in ζ direction is g_A g_B and g_C respectively.

$$g_A = \int_0^\infty P_n(\zeta)\frac{P^2(\zeta)}{1+m\zeta} d\zeta \cdots\cdots\cdots\cdots (17)$$

$$g_B = \int_0^\infty P_n(\zeta)P^2(\zeta)d\zeta \cdots\cdots\cdots\cdots\cdots (18)$$

$$g_C = \int_0^\infty P_n(\zeta)\frac{P^2(\zeta)}{\zeta}d\zeta \cdots\cdots\cdots\cdots (19)$$

In Eqs.(17)~(19), $P_n(\zeta)$ is a polynomial relating to ζ. When $\alpha > 0$, it is obvious that g_A and g_B are convergent, while g_C can be written as

$$g_C = \int_0^\infty P_n(\zeta)\frac{P^2(\zeta)}{\zeta}d\zeta$$
$$= g_0 + \int_0^\infty P_0 \frac{P^2(\zeta)}{\zeta}d\zeta \cdots\cdots\cdots\cdots (20)$$

in which g_0 is a convergent generalized integration, P_0 is a constant. Thus, the convergence of g_C depends on the integration $\int_0^\infty P_0 \dfrac{P^2(\zeta)}{\zeta} d\zeta$. It is easily proved, in the case of $P_0 \neq 0$, that $\int_0^\infty P_0 \dfrac{P^2(\zeta)}{\zeta} d\zeta$ is divergent. For C-type element, P_0 is the quantity relating to the mid-nodes of infinite elements and the material properties, and in general, $P_0 \neq 0$. Hence g_C is divergent. It indicates that we must avoid using C-type infinite elements in practical reckoning if mapping and shape functions are adopted as Eqs.(9) and (10) respectively.

The integration in η direction can be expressed as

$$\int_{-1}^1 Q_n(\eta) \frac{1}{\det[J]} d\eta$$

where $Q_n(\eta)$ is a polynomial relating to η. From Eqs.(13)~(16), we have : $-1 < \eta < 1 \rightarrow \det[J] \neq 0$. Hence the integration in η direction can be calculated by the Gaussian Integration Formula.

(2) **numerical integration scheme**

For the generalized integration in ζ direction, Ref.16). gives the Newton-Cotes Formula, which is also adopted in Ref.12) and Ref.13) as follows

$$g = \int_0^\infty f(\zeta) e^{-2(\alpha+i\beta)\zeta} d\zeta = \sum W_i f(\zeta_i) \quad \cdots\cdots (21)$$

The four point integration with $\zeta = 2, 4, 6, 8$, is chosen and thus the related weighting coefficients are as follows :

$$\left.\begin{array}{l} W_1 = \dfrac{1}{24}(96\nu - 52\nu^2 + 18\nu^3 - 3\nu^4) \\[2mm] W_2 = \dfrac{1}{8}(-48\nu + 38\nu^2 - 16\nu^3 + 3\nu^4) \\[2mm] W_3 = \dfrac{1}{8}(32\nu - 28\nu^2 + 14\nu^3 - 3\nu^4) \\[2mm] W_4 = \dfrac{1}{24}(-24\nu + 22\nu^2 - 12\nu^3 + 3\nu^4) \end{array}\right\} \cdots (22)$$

where

$$\nu = \frac{1}{2}\left(\frac{\alpha - i\beta}{\alpha^2 + \beta^2}\right) \quad \cdots\cdots\cdots\cdots\cdots (23)$$

Note that the function $f(\zeta)$ in Eq.(21) must be a polynomial, hence Eq.(21) is only used to calculate the stiffness matrices of B-type element.

For A-type element, we can acquire another generalized integration's numerical calculation formula :

$$\int_0^\infty P_n(\zeta) \frac{P^2(\zeta)}{1+m\zeta} d\zeta = \sum W_i^m P_n(\zeta_i) \quad \cdots\cdots (24)$$

where m is a positive real number, and A-type

infinite element stiffness matrices can be computed by Eq.(24).

The number of integration points in the ζ direction is related to the function $P_n(\zeta)$. Based on mapping and shape functions of infinite elements, $P_n(\zeta)$ is a polynomial with a power not greater than 2. Thus the four point integration with $\zeta = 2, 4, 6, 8$ is chosen, and the corresponding weighted coefficients are :

$$\left.\begin{array}{l} W_1^m = \dfrac{1}{48}(p_{11}\nu^3 + p_{12}\nu^2 + p_{13}\nu + p_{14}p_m) \\[2mm] W_2^m = \dfrac{1}{16}(p_{21}\nu^3 + p_{22}\nu^2 + p_{23}\nu + p_{24}p_m) \\[2mm] W_3^m = \dfrac{1}{16}(p_{31}\nu^3 + p_{32}\nu^2 + p_{33}\nu + p_{34}p_m) \\[2mm] W_4^m = \dfrac{1}{48}(p_{41}\nu^3 + p_{42}\nu^2 + p_{43}\nu + p_{44}p_m) \end{array}\right\} \cdots (25)$$

where

$$p_m = \int_0^\infty \frac{P^2(\zeta)}{1+m\zeta} d\zeta \cdots\cdots\cdots\cdots\cdots\cdots (26)$$

$$p_{11} = -\frac{2}{m} \cdots\cdots\cdots\cdots\cdots\cdots\cdots\cdots (27\,a)$$

$$p_{12} = \frac{18}{m} + \frac{1}{m^2} \cdots\cdots\cdots\cdots\cdots\cdots (27\,b)$$

$$p_{13} = -\left(\frac{104}{m} + \frac{18}{m^2} + \frac{1}{m^3}\right) \cdots\cdots\cdots (27\,c)$$

$$p_{14} = 192 + \frac{104}{m} + \frac{18}{m^2} + \frac{1}{m^3} \cdots\cdots\cdots (27\,d)$$

$$p_{21} = \frac{2}{m} \cdots\cdots\cdots\cdots\cdots\cdots\cdots\cdots (27\,e)$$

$$p_{22} = -\left(\frac{16}{m} + \frac{1}{m^2}\right) \cdots\cdots\cdots\cdots\cdots (27\,f)$$

$$p_{23} = \left(\frac{76}{m} + \frac{16}{m^2} + \frac{1}{m^3}\right) \cdots\cdots\cdots\cdots (27\,g)$$

$$p_{24} = -\left(96 + \frac{76}{m} + \frac{16}{m^2} + \frac{1}{m^3}\right) \cdots\cdots (27\,h)$$

$$p_{31} = -\frac{2}{m} \cdots\cdots\cdots\cdots\cdots\cdots\cdots\cdots (27\,i)$$

$$p_{32} = \frac{14}{m} + \frac{1}{m^2} \cdots\cdots\cdots\cdots\cdots\cdots (27\,j)$$

$$p_{33} = -\left(\frac{56}{m} + \frac{14}{m^2} + \frac{1}{m^3}\right) \cdots\cdots\cdots (27\,k)$$

$$p_{34} = 64 + \frac{56}{m} + \frac{14}{m^2} + \frac{1}{m^3} \cdots\cdots\cdots (27\,l)$$

$$p_{41} = \frac{2}{m} \cdots\cdots\cdots\cdots\cdots\cdots\cdots\cdots (27\,m)$$

$$p_{42} = -\left(\frac{12}{m} + \frac{1}{m^2}\right) \cdots\cdots\cdots\cdots\cdots (27\,n)$$

$$p_{43} = \frac{44}{m} + \frac{12}{m^2} + \frac{1}{m^3} \cdots\cdots\cdots\cdots\cdots (27\,o)$$

$$p_{44} = -\left(48 + \frac{44}{m} + \frac{12}{m^2} + \frac{1}{m^2}\right) \quad \cdots\cdots\cdots (27\,\mathrm{p})$$

The generalized integration

$p_m = \int_0^\infty \frac{P^2(\zeta)}{1+m\zeta} d\zeta = \int_0^\infty \frac{e^{-2(\alpha+i\beta)\zeta}}{1+m\zeta} d\zeta$ can be trans-

formed into series calculate[17].

$$p_m = \frac{1}{m} e^{Z_m} \int_1^\infty \frac{e^{-z_m t}}{t} dt = \frac{1}{m} e^{Z_m}$$

$$\int_{Z_m}^\infty \frac{e^{-x}}{x} dx = \frac{1}{m} e^{Z_m} E_1(Z_m) \quad \cdots\cdots\cdots (28)$$

$$E_1(Z_m) = -0.5772156649$$

$$-\ln Z_m - \sum_{n=1}^\infty \frac{(-1)^n Z_m^n}{n\,n!} \quad \cdots\cdots\cdots (29)$$

in which

$$Z_m = \frac{2(\alpha+i\beta)}{m} \quad \cdots\cdots\cdots\cdots\cdots\cdots (30)$$

If we stipulate that m equals 1 for B-type element, it may be easily verified that integration g_B can be calculated by Eq.(24)

$$g_B = \int_0^\infty P_n(\zeta) P^2(\zeta) d\zeta = \int_0^\infty P_n(\zeta)$$

$$(1+m\zeta) \frac{P^2(\zeta)}{1+m\zeta} d\zeta$$

$$= \sum W_i^m P_n(\zeta_i)(1+m\zeta_i)$$

$$= \sum W_i^m (1+m\zeta_i) P_n(\zeta_i)$$

Hence Eq.(24) can be regarded as the popularization of Eq.(21). g_A and g_B-type integrations can be reckoned by the general form's numerical formula.

$$g_{AB} = \int_0^\infty f(\zeta) P^2(\zeta) d\zeta = \sum W_i^m$$

$$(1+m\zeta_i) f(\zeta_i) = \sum U_i^m f(\zeta_i) \quad \cdots\cdots\cdots (31)$$

in which

$$U_i^m = W_i^m (1+m\zeta_i) \quad \cdots\cdots\cdots\cdots\cdots (32)$$

$$f(\zeta) = \frac{P_n(\zeta)}{1+m\zeta} \quad (m>0)$$

Because infinite element mass matrices have the forms of the g_B-type integration, we can calculate them with Eq.(31). Thus Eq.(31) is a general formula for calculation of stiffness and mass matrices of the two-dimensional dynamic infinite elements. Because the series in Eq.(29) is fast convergent, the Eq. (31) is very efficient. It is worth pointing out that a satisfied result can not be got by using the numerical methods in Ref. 18) for g_A-type integration.

3.　NUMERICAL VERIFICATION

According to the above-mentioned analysis procedures and formulations, a computer program
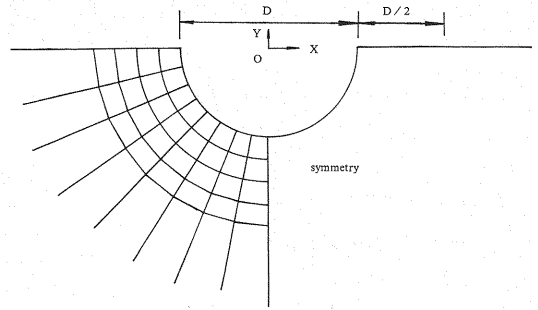

Fig.4 A test example about semi-circular canyon response

(a)　vertically incident P wave
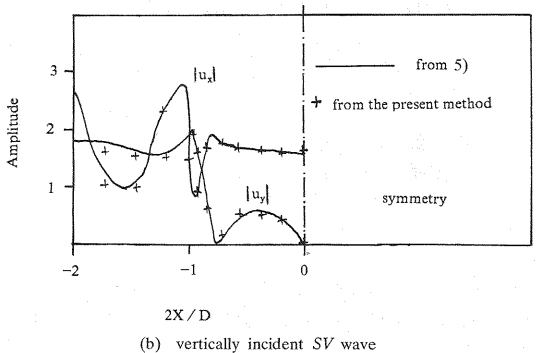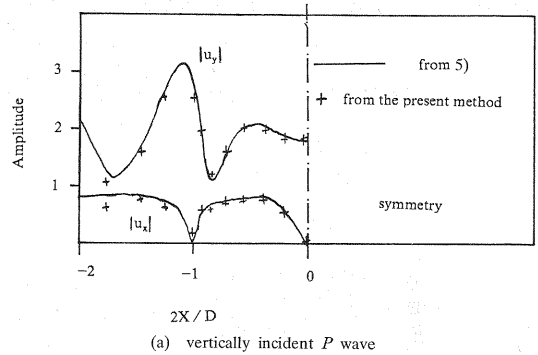

(b)　vertically incident SV wave

Fig.5 A comparison of displacement amplitudes at the surface of a canyon from the present method and from 5).

was developed to solve the free field response of a canyon. To verify the accuracy of the program, a comparison was made with previously obtained solutions[5], in which a semi-circular canyon in a homogeneous half space under vertically propagating harmonic P and S waves is employed (**Fig.4**). In the analysis, the ratio of canyon's width to the shear wavelength r_s takes 1.5, and 64 finite elements and 16 infinite elements are adopted. The present results are ploted in **Fig.5**. It shows a good agreement to the results obtained by the generalized inverse methods[5].
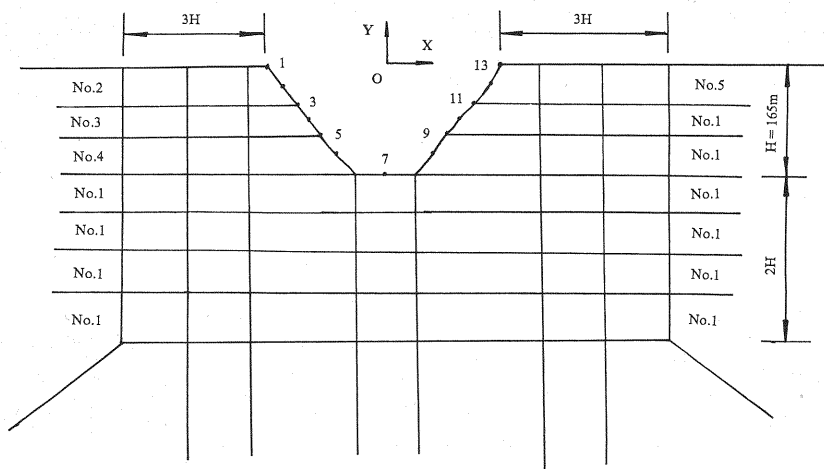
Fig.6 The calculation model of the Li Jia Xia Arch Dam Canyon free-field motions

Table 1 The Material properties

Material Number	No.1	No.2	No.3	No.4	No.5
Elastic Modulus E(MPa)	0.2000	0.1030	0.1725	0.1800	0.1403

4. ENGINEERING APPLICATION

A practical example of the use of above-mentioned procedures in large dam engineering is shown in **Fig.6**.

The Li Jia Xia Arch Dam on the Yellow River lies Qinghai Province, Northwest China, with a height of 165 m above the rock foundation. The Dam Valley is a V-shape canyon as shown in **Fig.6**, the two sides of valley lie in the rock of different material properties (**Table 1**). But the material's difference on the two sides is very small, the canyon can be approximately simulated by the model as shown in **Fig.1**, so the method presented in this paper can be used to solve the Li Jia Xia Canyon's free field motions. In the analysis, we adopt three practical earthquake records that are Koyna (1967, India), Song Pan (1976, China) and Qian An (1976, China) respectively, but with the maximum peak acceleration 0.2 g according to the Chinese Seismic Design Regionalization Map, and it is assumed that the motions of the depth of the base rock at record station is equal to ones at canyon site. So the deconvolved analysis should be performed, i.e, a measured earthquake acceleration is deconvolved to the depth of the base, the deconvolved waves are obtained, and the input compoments of the deconvolved waves are used as the incident waves of free field calculating model of the Li Jia Xia Canyon (convolved analysis). The
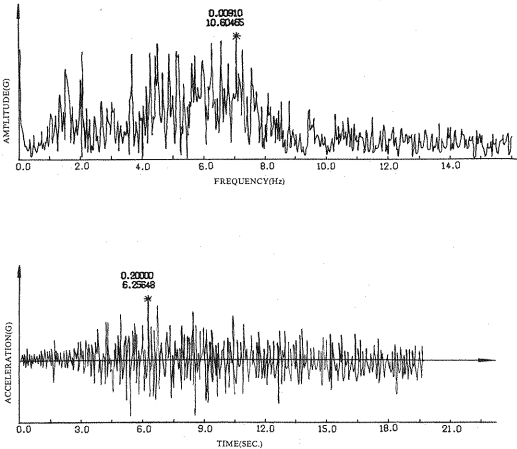

Fig.7 The X direction Song Pan earthquake wave and its Fourier spectrum

deconvolved analysis was also presented in Ref. 20), its basic formulations have been given in above-mentioned the response of w subsystem.

The X direction component of Song Pan earthquake accelerograms and Fourier spectrum are presented in **Fig.7**, the corresponding deconvolved wave input component and Fourier spectrum are given in **Fig.8**, and the corresponding canyon acceleration histories and Fourier spectrums are shown in **Fig.9, 10** for stations 1 and 7 recpectively. The X direction responses of the
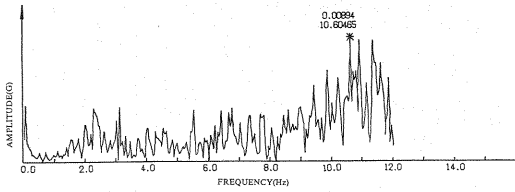
Fig.8 The X direction input component of Song Pan deconvolved waves and its Fourier spectrum.
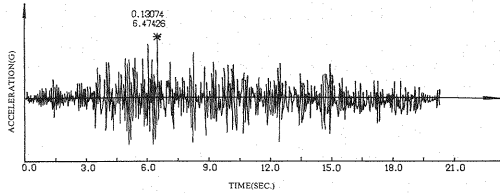

Fig.9 The X direction acceleration history and Fourier spectrum of station 1 under Song Pan input wave.
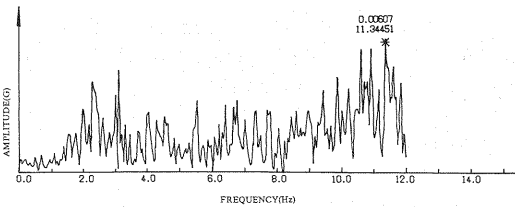

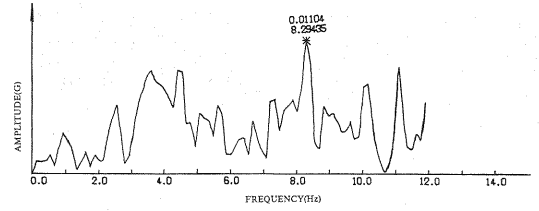**Fig.10** The X direction acceleration history and Fourier spectrum of station 7 under Song Pan input wave.

Fig.11 The X direction acceleration history and Fourier spectrum of station 1 under Qian An input wave.
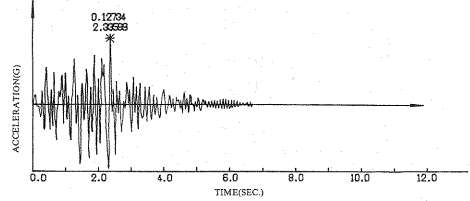

Fig.12 The X direction acceleration history and Fourier spectrum of station 1 under Koyna input wave.

canyon to Koyna and Qian An earthquake input waves are also presented in **Figs.11, 12** for stations 1.

Under different input waves, the response maximum peak accelerations at different points are presented in **Table 2**. The X, Y and Z in **Table 2** represent across, vertical and downstream river direction respectively.

From the above-mentioned results, we may draw the following conclusions.

1) From time histories, there are some differences among the measured earthquake records, deconvolved waves and response accelerations at different nodes, and the differences in Fourier spectra are more obvious. It shows that both the amplitudes and frequency contents of accelerations are remarkably changed by deconvolution and canyon free field response analysis.

Table 2 The peak accelerations at dam canyon

Node No	Koyna			Qian An			Song Pan		
	X	Y	Z	X	Y	Z	X	Y	Z
1	−0.18172	0.20412	−0.19140	0.12734	0.21130	0.13188	0.12388	0.13048	0.13293
2	0.10072	0.16321	−0.14509	−0.08752	0.15746	−0.09821	−0.06077	0.10351	0.10725
3	−0.09990	−0.13473	−0.12595	−0.06624	0.12269	0.13123	0.06861	0.07894	−0.08918
4	−0.10872	0.13153	−0.12424	−0.06708	0.13667	0.13079	0.06901	0.08125	−0.07696
5	−0.09758	−0.11749	0.10132	−0.07929	0.12014	0.12020	0.08109	0.07069	0.07864
6	−0.13848	0.13768	−0.12734	0.09076	0.12887	0.13607	0.09425	0.07202	−0.08576
7	−0.16484	−0.14992	−0.14965	0.10259	0.15789	0.15359	0.10261	0.06628	0.08744
8	−0.14730	0.15063	−0.11639	−0.08197	0.14417	0.13497	0.09620	0.06119	−0.08124
9	−0.11948	0.16062	−0.10534	−0.06938	0.14959	0.13214	0.08650	0.06006	−0.07583
10	−0.11951	0.13315	−0.11735	−0.07681	0.14281	0.12157	0.06319	0.06518	−0.07442
11	−0.09686	0.15567	−0.13228	−0.07475	0.13869	0.10471	0.06105	0.06858	0.08572
12	0.09106	0.17874	0.13229	−0.09979	0.16864	0.09419	0.06312	−0.07533	0.10833
13	−0.17713	0.20402	−0.17662	−0.12623	0.21021	−0.12056	0.11063	−0.08414	0.11385

2) For different earthquake patterns with the same 0.2 g peak acceleration, the response peak accelerations at the same node are different. It shows that the time histories of the earthquake records have a great influence on canyon free-field motion.

3) For the same input waves, the response peak accelerations at the different nodes are different, and ones at canyon middle level take minimum. It shows that canyon free-field motion distributions are not uniform. The ratio of the peak accelerations at top points to bottom point 7 is about 1 to 1.5.

5. CONCLUSIONS

The analysis method presented in this paper is suitable for solving the free field seismic motion of a two-dimensional canyon for vertically incident P and S waves, in which the coupling model of finite element and infinite element is adopted. The present method is one of alternatives in the calculation of the free field response of a canyon.

REFERENCES
1) R.W. Clough, K.T. Chang, H.Q. Chen, Y. Ghanaat : Dynamic Interaction Effects in Arch Dams, Report No. UBC/EERC-85/11, October, 1985.
2) M.D. Trifunac : Scattering of plane SH waves semi-cylindrical canyon, Earthquake eng. struct. dyn. 1, pp.267 ~281, 1973.
3) H.L. Wong and M.D. Trifunac : Scattering of plane *SH* waves by a semi-elliptical canyon, Earthquake eng. struct. dyn. 3, pp.157~169, 1974.
4) W.D. Smith : The application of finite element analysis to body wave propagation problems, J. geophys. 44, pp.747~ 768, 1975.
5) H.L. Wong : Effect of surface topography on the diffraction of P, SV, and Rayleigh waves, Bull. seism. soc.

Am. 72, pp.1167~1183, 1982.

6) H. Cao and V.W. Lee : Scattering and diffraction of plane P waves by circular cylindrical canyons with variable depth-to-width ratio, Soil dyn. earthquake eng. 9, pp.141 ~150, 1990.

7) R.F. Vogt, J.P. Wolf and H. Bachmann : Wave Scattering by a canyon of arbitrary shape in a layered half-space, Earthquake eng. struct. dyn. 16, pp.803~812, 1988.

8) L. Zhang and A.K. Chopra : Three-dimensional analysis of spatially varying ground motions around a uniform canyon in a homogeneous half-space, Earthquake eng. struct. dyn., 20, pp.911~926, pp.1991.

9) P. Bettess : Infinite elements, Int. J. Num. Meth. Eng. 11, pp.53~64, 1977.

10) Zienkiewicz, O.C, Bettess, P. : Infinite element in study of fluid-structure interaction problems, Second Int. Symp. in Computing Methods in Applied Science Engineering, IRIA, Versailles, France, 1975.

11) Beer, G. : Infinite domain elements in finite element analysis of underground excavations, Int. J. Num. and Ana. Meth. Geo. 17, pp.1~7, 1983.

12) Zhang Chuhan and Zhao Chongbin : Coupling method of finite and infinite elements for strip foundation wave problems, Earthquake eng. struct. dyn. 15, pp.839~851.

1987.

13) Zhang Chuhan and Zhao Chongbin : Effects of canyon topography and geological conditions on strong ground motion, Earthquake eng. struct. dyn. 16, pp81~97, 1988.

14) J.P. Wolf, Dynamic Soil-Structure Interaction, Prentice-Hall, Englewood Cliffs, N.J., 1985.

15) O.C. Zienkiewicz : The Finite Element Method, McGraw-Hill, New York, 3 rd edn, 1977.

16) Y.K. Chow and I.M. Smith : Static and periodic soid elements, Int. J. Num. Meth. Eng. 17, pp.503~526, 1981.

17) Milton Abramowitz and Iren. A. Stegun : Handbook of Mathematical Functions with Formulas Graphs and Mathematical Tables' New York, Dover Pub. Inc. 1972.

18) P.J. Davis and P. Rabinowitz : Methods of Numerical Integration, Academic Press, New York, 1975.

19) Pre B. Schnable, John Lysmer, H. Bolton Seed : SHAKE-A Computer Program for Earthquake Response Analysis of Horizontally Layered Site, University of California, Berkeley, Earthquake Engineering Center, Report No. UCB/EERC-72/12, 1972.

20) Chen Houqun, Wang Jun : Free field seismic motions at arch dam canyon, China-US Workshop on Earthquake Behavior of Arch Dams. Beijing, China, June 1987.

(Received May 12, 1992)